JACS
JOURNAL OF THE AMERICAN CHEMICAL SOCIETY

Communication

pubs.acs.org/JACS

Directional Synthesis and Assembly of Bimetallic Nanosnowmen with DNA

Jung-Hoon Lee, Gyeong-Hwan Kim, and Jwa-Min Nam*

Department of Chemistry, Seoul National University, Seoul 151-747, Korea

Supporting Information

ABSTRACT: Synthesizing and assembling nanoscale building blocks to form anisotropic nanostructures with the desired composition and property are of paramount importance for the understanding and use of nanostructured materials. Here we report a salt-tuned synthetic strategy using DNA-modified Au nanoparticles (DNA-AuNPs) to form Au–Ag head–body nanosnowman structures in >95% yield. We propose a mechanism for the formation of asymmetric Au–Ag nanosnowmen from DNA-AuNPs, salts, and Ag-precursor-loaded polymers. Importantly, we show that oriented assemblies of various nanostructures are readily obtained using nanosnowmen with asymmetrically modified DNA as building blocks.

Because of their plasmonic, catalytic, electronic, and magnetic properties, metal nanostructures have been intensively studied over the past decade.[1] Combining multiple metallic nanocomponents into a single specific nanostructure often generates unusual optical and chemical properties (e.g., intense plasmonic coupling and higher chemical affinity) and offers wider and more diverse applications.[1b,2] However, synthesizing and assembling these complex nanostructures are challenging, and the use of multicomponent, multimeric metallic nanostructures is severely limited because of their synthetic inaccessibility. Although there has been much progress in synthesizing various nanostructures, including multimetallic core–shell nanoparticles (NPs), tadpole-like structures, heterodimers, and nanopolyhedra and nanorods, most reported methods for synthesizing heterometallic hybrid NPs involve complicated procedures and harsh reaction conditions.[1,2] Furthermore, although highly challenging, asymmetric syntheses of complex nanostructures with specific orientations could lead to materials with unprecedented properties and functions.[3−5]

Here we report a DNA-based approach for the synthesis of Au–Ag head–body "nanosnowman" particles in a high yield (>95%) by simple control of the salt concentration (NaCl in this case) under aqueous conditions (Figure 1). The asymmetric growth of a silver NP (AgNP) on the surface of a DNA-modified gold NP (DNA-AuNP) was observed as a lower salt concentration was applied to the reaction solution. Importantly, we have shown that these nanosnowman particles with asymmetrically modified DNA can be used as building blocks for the oriented assembly of various complex nanostructures. Typically, when Ag-shell-forming agents are added to DNA-AuNPs, spherical Au–Ag core–shell structures

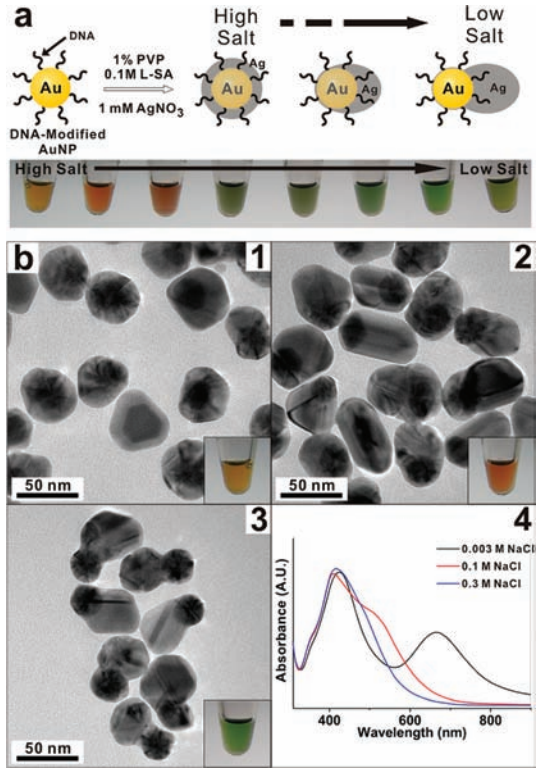

Figure 1. (a) Schematic illustration and solution color images of Au–Ag nanostructures with varying salt concentration. (b) (1–3) HRTEM images of NPs synthesized at salt concentrations of (1) 0.3, (2) 0.1, and (3) 0.003 M and (4) the corresponding UV–vis spectra.

are formed.[6] However, here we have found that anisotropic Au–Ag head–body nanosnowman structures can be obtained simply by lowering the salt concentration and adding a proper reducing agent and polymer for the process of AgNP budding on the DNA-AuNP surface. DNA on the AuNP surface offers high particle stability, efficient surface protection, and controllability of oriented particle growth. It should also be noted that the reaction rate for Ag growth on the Au surface was much higher at lower salt concentrations and that salts can reduce the repulsive force between the DNA strands on AuNPs,[7] suggesting that lower salt concentrations free the space between DNA strands on the AuNP surface and allow Ag precursors to be harnessed on the nucleation sites more readily.

Received: December 29, 2011
Published: March 6, 2012

dx.doi.org/10.1021/ja2121525 | J. Am. Chem. Soc. 2012, 134, 5456–5459

Interestingly, as a result of this asymmetric growth, DNA strands were buried on the side with Ag growth, while the other Au surface without Ag budding had exposed DNA that could hybridize. These nanosnowman particles with asymmetrically modified DNA can offer platforms for DNA-based assembly of various aligned and unconventional nanostructures.

In a typical experiment, first, the nanosnowman structures were synthesized by using DNA-AuNPs as seeds and adding Ag precursors and other reagents to grow Ag structures on the DNA-AuNP surface with control over the salt concentration. The asymmetric structure growth process started with modification of AuNPs with thiolated DNA [see the Supporting Information (SI) for details]. The resulting DNA-AuNPs were then used as seeds for the asymmetric AgNP growth on the DNA-AuNP surface. A polymer-aided chemical reduction method involving poly(vinylpyrrolidone) (PVP), (+)-sodium L-ascorbate (L-SA), and $AgNO_3$ in deionized water was used to form the Au–Ag head–body nanosnowman structures. The PVP, L-SA, and Ag precursors were added sequentially to the DNA-AuNP seed solution (see the SI).

When the salt concentration was varied from high to very low values (0.3, 0.1, and 0.003 M NaCl), different solution colors ranging from yellow to orange, dark-green, and bright-green were observed (Figure 1a), along with a structural transformation from spherical Au–Ag core–shell particles to Au–Ag head–body nanosnowman particles. The formed nanostructures were confirmed by high-resolution transmission electron microscopy (HRTEM) and UV–vis spectroscopy. The HRTEM images of nanostructures obtained from reactions with different salt concentrations show the structural changes from spherical particles to snowmanlike nanostructures (Figure 1b, panels 1–3). The UV–vis data (Figure 1b, panel 4) show that the plasmonic peaks of the nanostructures were strongly affected by varying the salt concentration, with a new plasmonic band appearing at ~650 nm at a very low salt concentration (0.003 M). In general, the intensity of the resonance peak increases when charges separate with mirror symmetry because this provides the main restoring force for electron oscillation. Therefore, in general, the intensity of the longitudinal peak is higher than that of the transverse peak because of the increase in the effective dipole moment of the particle, which is larger if charges separate with mirror symmetry. One possible reason why the amplitude of the longitudinal band is lower than that of transverse mode in our case is that mirror symmetry of a nanosnowman structure is not fully isotropic, and the Au–Ag bimetal composition could also affect the anisotropy of the mirror symmetry.[8,9] Asymmetric Ag growth on the surfaces of the AuNPs can be clearly seen in the images in panels 2 and 3 in Figure 1b, but snowman nanostructures were more reproducibly grown in a much higher yield for the very low salt case (Figure 1b, panel 3). The lengths of the longest axes for the spherical core–shell, intermediate nanosnowmen, and nanosnowmen were approximately 46, 50, and 64 nm, respectively (200 particles were measured for each case). The TEM results for the structural changes were well-matched with the UV–vis results, which showed that the appearance of the surface plasmon resonance (SPR) bands changed from that for a spherical shape to that for rod or dimeric shapes as the salt concentration decreased (Figure 1b, panel 4). Secondary SPR modes, which are associated with the longitudinal axis, are known to shift to longer wavelengths as the NP shape gets longer.[1e]

Next, we studied the salt-dependent reaction kinetics by UV–vis spectroscopy to investigate the reaction mechanism and the roles of DNA and salt concentration. While the salt concentration was altered, the same amounts of PVP, L-SA, and Ag precursors as well as the same temperature (room temperature) were used and maintained for all of the experiments. Figure 2 shows changes in the absorbance at

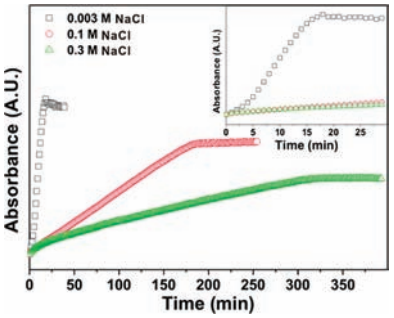

Figure 2. Salt-dependent reaction kinetics. The results for 0.3, 0.1, and 0.003 M NaCl were obtained by using the UV–vis spectrophotometer. The inset shows the magnified area from 0 to 30 min reaction time.

400 nm as a function of time for three cases with different salt concentrations (0.3, 0.1, and 0.003 M NaCl). The UV–vis spectra were measured at 1 min intervals. Overall, the results show that the reaction rate drastically increased as the salt concentration decreased from 0.3 to 0.003 M. The times required for reaction completion were approximately 15 min, 3 h, and 5 h for 0.003, 0.1, and 0.3 M NaCl, respectively. Reaction was completed very fast, especially at very low salt concentration (Figure 2 inset). This fast kinetics for 0.003 M NaCl in forming nanosnowman particles suggests that fast nucleation and growth of Ag on the AuNP surface is critical in forming a specific nanostructure in a high yield and that a low salt concentration facilitates this process. In the case of nearly no salt condition (<1 nM), the reaction was finished within ~2 min. TEM image analysis showed that nanosnowman structures were formed only partially and that many other structures, including spherical core–shell particles and irregularly shaped nanostructures, were also formed as a result of the uncontrollably fast reaction kinetics (Figure S1 in the SI). These results suggest that low concentration is preferred for faster kinetics and formation of uniform nanosnowman structures in a high yield but also that the reaction becomes uncontrollable and generates rather random nanostructures when there is nearly no available salt in solution.

We also performed reactions using AuNPs without DNA modification at two different salt concentrations (0.003 M and no salt) to see the effect of DNA and its correlation with the presence of salt. Without salt, the reaction was finished within a few seconds, and Ag structures were grown and budded from AuNP surface in many different directions with irregular shapes (Figure S2a). With 0.003 M salt, although the reaction rate was slowed (~15 min) and more directional growth of Ag from AuNP surface was observed, no particular structure with a defined shape was synthesized without DNA (Figure S2b). These results show that the presence of DNA on the AuNP surface is critical in forming nanosnowman structures in a high yield in a controllable fashion and again that salt adjustment is an important handle to drive the directional growth of Ag structures on AuNP surfaces. To confirm the influence of poly(ethylene glycol) (PEG) or DNA sequences on Ag growth,

dx.doi.org/10.1021/ja2121525 | J. Am. Chem. Soc. 2012, 134, 5456–5459

we tested five different DNA sequences (A_{30}-SH, A_{10}-SH, T_{30}-SH, and T_{10}-SH for the DNA sequence effect and 15-mer-PEG-A_{10}-SH and 15-mer-A_{10}-SH for the PEG effect; Figures S3 and S4). It should be noticed that A binds more strongly to the Au surface than T and that poly-A DNA results in a smaller amount of loading per AuNP than poly-T DNA.[10] The resulting nanosnowman structures were similar, but poly-A generated faster kinetics than poly-T (Figure S3). This becomes more clear because the longer A_{30} or T_{30} sequence induced faster kinetics than the A_{10} or T_{10} sequence. In the case of PEG, the number of modified DNA per AuNP was increased by inserting PEG into the thiolated DNA sequence.[7] Our results show that addition of PEG slows the Ag budding kinetics (Figure S4). We next examined the role of PVP. Without PVP, Ag deposition on the AuNP surface did not occur. It is well-known that PVP can harness and carry Ag^+ ions via chelation by donation of lone-pair electrons of O or N atoms of PVP, forming coordination complexes in aqueous solution.[11] Furthermore, Ag^+ can form precipitates of AgCl without PVP because there are many Cl^- ions in our system, but no precipitates were observed in solution.

On the basis of these results and previous knowledge, we proposed the following reaction mechanism for asymmetric growth of Ag nanostructures on AuNP surfaces to form Au−Ag nanosnowmen (Figure 3a). It is well-known that salts can

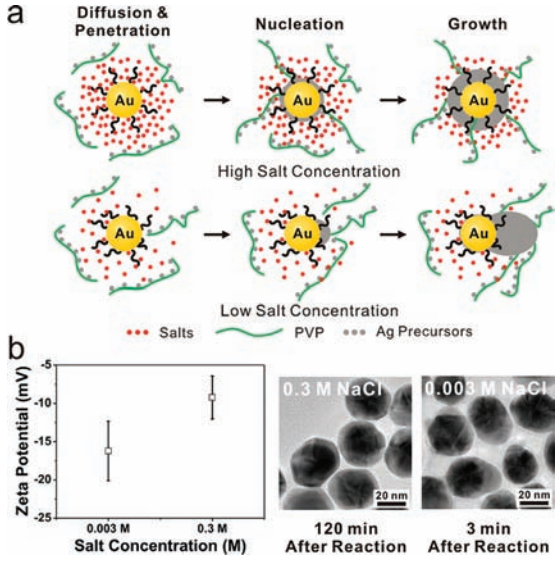

Figure 3. (a) Proposed reaction mechanism at different salt concentrations. (b) ζ potentials for DNA-AuNPs at 0.003 and 0.3 M salt concentration (left); HRTEM images of Ag nanostructure formation on DNA-AuNPs at intermediate stages (right).

reduce the repulsive forces between DNA strands, increase the DNA loading on the AuNP surface, and induce more straightened and uniform DNA structures.[7] At a lower salt concentration, a smaller amount of salt exists around the AuNPs and less uniform DNA structures are formed on the AuNP surface. The salt distribution and DNA structures on AuNPs are critical factors in Ag structure growth on DNA-AuNPs, especially when Ag precursors are carried by bulky PVP to the AuNP surface for nucleation and subsequent Ag structure growth. At high salt concentration (Figure 3a, top scheme), salt can be densely packed around the DNA-AuNPs to form a passivation layer, and the DNA strands are rather uniformly distributed around the AuNPs. Thus, at high salt concentration, it is difficult for Ag−PVP complexes to penetrate through this salt layer, and slower reaction kinetics is observed. As a result of the uniformity of the DNA structures, multiple nucleation sites formed slowly and simultaneously, affording Au−Ag core−shell nanospheres. In contrast, at low salt concentration (Figure 3a, bottom scheme), less uniform DNA structures can be formed on the AuNP surface, facilitating the introduction of Ag−PVP in a certain direction, and a less dense, imperfect salt layer is formed around the DNA-AuNPs. Ag−PVP complexes can more readily approach the AuNP surface, and once an Ag nucleation site forms, Ag in approaching Ag−PVP complexes should be preferentially deposited at the already-formed Ag site, resulting in faster reaction kinetics and directional growth of the Ag nanostructure on the AuNP surface. The ζ potential was more negative at lower salt concentration (Figure 3b), and taking into account that DNA phosphate backbones are negatively charged and salt between the DNA strands creates a charge-screening effect, the results suggest that a smaller amount of salt is distributed around the DNA-AuNPs at lower salt concentration. Furthermore, there is less Cl^- ion at the low salt concentration, which could affect the chemical equilibrium ($Ag^+ + Cl^- \rightleftarrows AgCl$). The proposed mechanism is further supported by the HRTEM images of particles during intermediate stages (120 and 3 min after reaction initiation using 0.3 and 0.003 M NaCl, respectively; Figure 3b). The TEM images show that the Ag shell grew rather uniformly all around the Au surface for 0.3 M NaCl, while an asymmetric Ag budding process was observed for the case of 0.003 M NaCl. During the growth step, the reduction of Ag precursors occurs preferentially at the nucleation sites, as it is much easier for Ag to be deposited on a pre-existing nucleation site after the initial nucleation step.[2c,e]

One can readily notice that DNA-nanosnowman particles have not only asymmetrically grown nanostructures but also asymmetric DNA modification on their surfaces. On the Au head side, DNA is exposed and can be readily hybridized to complementary DNA (cDNA). On the other hand, on the Ag body side, the DNA is buried within the Ag structure, and cDNA coupling is not possible (Figure 4a). Using this asymmetric feature, one can implement directional assemblies of various unique nanostructures. First, we added single $cDNA_2$-modified AuNPs [13 nm in diameter, Au-5′-HS-$(CH_2)_6$-A_{10}-PEG_{18}-ATCCTTATCAATATT-3′; see the SI for details] to DNA_1-nanosnowmen [5′-TAACAATAATCCCTC-PEG_{18}-A_{10}-$(CH_2)_3$-SH-3′-Au]. In a typical experiment, an excess amount of linker DNA (5′-GAGGGATTATTGTTAAA-TATTGATAAG-GAT-3′, 10 000-fold higher amount than AuNP concentration), which links two half-cDNA-modified NPs, was used to hybridize the DNA-modified NPs in 0.15 M PBS solution (see the SI for details). Panel 1 in Figure 4b shows HRTEM images of structures assembled with DNA_1-nanosnowmen and single $cDNA_2$-modified AuNPs. These results show that the 13 nm AuNPs are specifically assembled to the Au head regions. When $cDNA_2$-modified AuNPs (30 nm in diameter) were added to DNA_1-nanosnowmen, oriented assemblies of various nanostructures were observed via preferential binding of AuNPs to Au head parts in nanosnowmen (Figure 4b, panel 2). Finally, DNA_2-nanosnowmen and linker DNA were added to DNA_1-nanosnowmen (see the SI for details). Again, highly oriented nanoassembly structures were formed via preferential binding between Au head parts of DNA-

dx.doi.org/10.1021/ja2121525 | J. Am. Chem. Soc. 2012, 134, 5456−5459

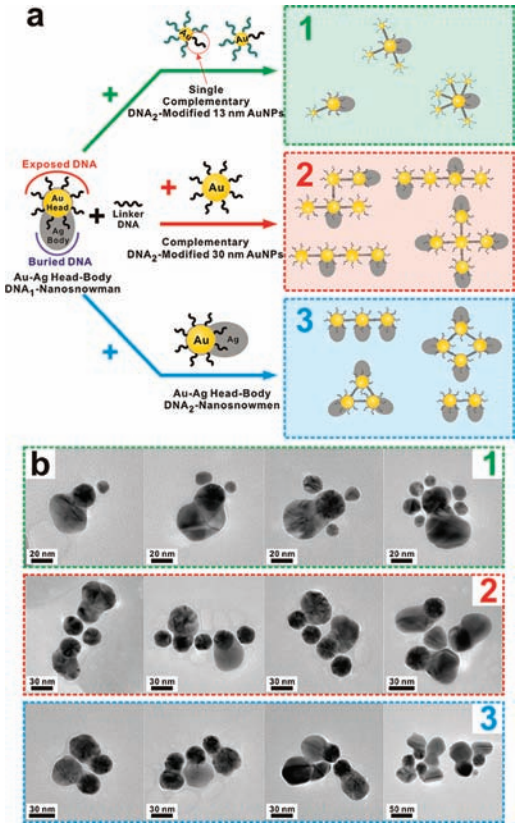

Figure 4. (a) Schematic illustration of the processes for directional assembly of DNA-nanosnowmen with asymmetric DNA modification. (b) HRTEM images of the assembled nanostructures.

nanosnowman particles (Figure 4b, panel 3). The UV–vis spectra were affected by the formation of oriented particle assemblies: the maximum signal intensities were decreased, and the peaks were distributed more broadly as a result of the formation of various aggregates (Figure S5).

In summary, we have reported a high-yield (>95%) synthetic approach for anisotropic bimetallic nanosnowman particles by lowering the salt concentration and using DNA-AuNPs as seeds. The salt concentration strongly affects the reaction kinetics, and much faster kinetics was observed at lower concentration. At very low salt concentration (0.003 M NaCl in this case), the reaction was complete within 15 min, suggesting that fast nucleation and growth of Ag on the AuNP surface is critical in forming a DNA-modified anisotropic metal nanostructure in a high yield and that a low salt concentration facilitates this process. We also found that the formation of Ag–PVP complexes is critical for the formation of nanosnowman structures. On the basis of these observations along with other characterization data, we have proposed a synthetic mechanism for these nanosnowman structures. Importantly, using asymmetrically modified DNA on the nanosnowmen, with exposed DNA on the Au head part and buried DNA on the Ag body part, we have produced oriented assemblies of nanostructures via highly preferential binding of Au head parts from the Au–Ag head–body nanosnowmen to form various nanostructures with directionality. The strategies and results herein provide a new pathway for the synthesis of anisotropic nanostructures in high yield and insights into the oriented assembly of unconventional nanostructures that could be useful for chemistry, materials science, plasmonics, and nanoscience.

■ ASSOCIATED CONTENT

Ⓢ Supporting Information

Methods, materials, and supporting figures. This material is available free of charge via the Internet at http://pubs.acs.org.

■ AUTHOR INFORMATION

Corresponding Author

jmnam@snu.ac.kr

Notes

The authors declare no competing financial interest.

■ ACKNOWLEDGMENTS

J.-M.N. was supported by a National Research Foundation of Korea (NRF) grant funded by the Korean Government (MEST) (2011-0018198). This work was also partially supported by the Industrial Core Technology Development Program of the Ministry of Knowledge Economy (10033477).

■ REFERENCES

(1) (a) Peng, X. G.; Manna, L.; Yang, W. D.; Wickham, J.; Scher, E.; Kadavanich, A.; Alivisatos, A. P. *Nature* **2000**, *404*, 59. (b) Shi, W.; Zeng, H.; Sahoo, Y.; Ohulchanskyy, T. Y.; Ding, Y.; Wang, Z. L.; Swihart, M.; Prasad, P. N. *Nano Lett.* **2006**, *6*, 875. (c) Wu, Y.; Xiang, J.; Yang, C.; Lu, W.; Lieber, C. M. *Nature* **2004**, *430*, 61. (d) Huang, M. H.; Mao, S.; Feick, H.; Yan, H. Q.; Wu, Y. Y.; Kind, H.; Weber, E.; Russo, R.; Yang, P. D. *Science* **2001**, *292*, 1897. (e) Lassiter, J. B.; Aizpurua, J.; Hernandez, L. I.; Brandl, D. W.; Romero, I.; Lai, S.; Hafner, J. H.; Nordlander, P.; Halas, N. J. *Nano Lett.* **2008**, *8*, 1212.

(2) (a) Mokari, T.; Rothenberg, E.; Popov, I.; Costi, R.; Banin, U. *Science* **2004**, *304*, 1787. (b) Cozzoli, P. D.; Pellegrino, T.; Manna, L. *Chem. Soc. Rev.* **2006**, *35*, 1195. (c) Gu, H.; Yang, Z.; Gao, J.; Chang, C. K.; Xu, B. *J. Am. Chem. Soc.* **2005**, *127*, 34. (d) Seo, D.; Yoo, C. I.; Jung, J.; Song, H. *J. Am. Chem. Soc.* **2008**, *130*, 2940. (e) Gu, H.; Zheng, R.; Zhang, X.; Xu, B. *J. Am. Chem. Soc.* **2004**, *126*, 5664. (f) Lim, D.-K.; Jeon, K.-S.; Hwang, J.-H.; Kim, H.; Kwon, S.; Suh, Y. D.; Nam, J.-M. *Nat. Nanotechnol.* **2011**, *6*, 452.

(3) (a) Connolly, S.; Nagaraja, R.; Fitzmaurice, D. *J. Phys. Chem. B* **2000**, *104*, 4765. (b) Kanaras, A. G.; Wang, Z.; Bates, A. D.; Cosstick, R.; Brust, M. *Angew. Chem., Int. Ed.* **2003**, *42*, 191. (c) Shevchenko, E. V.; Talapin, D. V.; Murray, C. B.; O'Brien, S. *J. Am. Chem. Soc.* **2006**, *128*, 3620.

(4) (a) Sardar, R.; Heap, T. B.; Shumaker-Parry, J. S. *J. Am. Chem. Soc.* **2007**, *129*, 5356. (b) Chen, G.; Wang, Y.; Yang, M.; Xu, J.; Goh, S. J.; Pan, M.; Chen, H. *J. Am. Chem. Soc.* **2010**, *132*, 3644. (c) Li, W.; Camargo, P. H. C.; Au, L.; Zhang, Q.; Rycenga, M.; Xia, Y. *Angew. Chem., Int. Ed.* **2010**, *49*, 164.

(5) (a) Caswell, K. K.; Wilson, J. N.; Bunz, U. H. F.; Murphy, C. J. *J. Am. Chem. Soc.* **2003**, *125*, 13914. (b) Salem, A. K.; Chen, M.; Hayden, J.; Leong, K. W.; Searson, P. C. *Nano Lett.* **2004**, *4*, 1163. (c) Chen, M.; Guo, L.; Ravi, R.; Searson, P. C. *J. Phys. Chem. B* **2006**, *110*, 211. (d) Salant, A.; Amitay-Sadovsky, E.; Banin, U. *J. Am. Chem. Soc.* **2006**, *128*, 10006.

(6) (a) Lim, D.-K.; Kim, I.-J.; Nam, J.-M. *Chem. Commun.* **2008**, 5312. (b) Lim, D.-K.; Jeon, K.-S.; Kim, H. M.; Nam, J.-M.; Suh, Y. D. *Nat. Mater.* **2010**, *9*, 60.

(7) Hurst, S. J.; Lytton-Jean, A. K. R.; Mirkin, C. A. *Anal. Chem.* **2006**, *78*, 8313.

(8) Tan, S. J.; Campolongo, M. J.; Luo, D.; Cheng, W. *Nat. Nanotechnol.* **2011**, *6*, 268.

(9) Wiley, B. J.; Im, S. H.; Li, Z.-Y.; McLellan, J.; Siekkinen, A.; Xia, Y. *J. Phys. Chem. B* **2006**, *110*, 15666.

(10) Storhoff, J. J.; Elghanian, R.; Mirkin, C. A.; Letsinger, R. L. *Langmuir* **2002**, *18*, 6666.

(11) Zhang, Z.; Zhao, B.; Hu, L. *J. Solid State Chem.* **1996**, *121*, 105.